Article:
Chang, L, Daly, C, Miller, DM et al. (4 more authors) (2019) Permeabilised skeletal muscle reveals mitochondrial deficiency in malignant hyperthermia-susceptible individuals. British Journal of Anaesthesia, 122 (5). pp. 613-621. ISSN 0007-0912

https://doi.org/10.1016/j.bja.2019.02.010

Permeabilized skeletal muscle reveals mitochondrial deficiency in malignant hyperthermia susceptible individuals

Authors:
L Chang[1], C Daly[2], DM Miller[1], PD Allen[1], JP Boyle[3], PM Hopkins[1, 2], M-A Shaw[1]

1. Leeds Institute of Medical Research at St. James's, University of Leeds, Leeds, UK
2. Malignant Hyperthermia Unit, St James's University Hospital, Leeds, UK
3. Leeds Institute of Cardiovascular & Metabolic Medicine, University of Leeds, Leeds, UK

Contribution of authors

Conception and design of the study: PMH, MAS, JPB
Conduct of experiments and data collection: LC, JPB
Data analysis & interpretation: all authors
Drafting of manuscript: LC, PMH
All authors reviewed drafts of the manuscript and approved the final version

Abbreviated title: Mitochondrial function in malignant hyperthermia

Corresponding author: Philip M Hopkins, Leeds Institute of Medical Research at St. James's, St James's University Hospital, Leeds, LS9 7TF, United Kingdom. Phone +44 113 2065274, Fax +44 113 2064140. Email: p.m.hopkins@leeds.ac.uk

Disclosure of funding sources:
BJA/RCoA PhD studentship (MAS & PMH)
National Institutes of Health (NIH): National Institute of Arthritis, Musculoskeletal and Skin Diseases (2P01 AR-05235; PDA, PMH)

Declaration of interests

PMH is an Editorial Board Member of BJA.

Abstract

Background. Individuals genetically susceptible to malignant hyperthermia (MH) exhibit hypermetabolic reactions when exposed to volatile anaesthetics. Mitochondrial dysfunction has previously been associated with the MH-susceptible (MHS) phenotype in animal models but evidence of this in human MH is limited.

Methods. We used high resolution respirometry to compare oxygen consumption rates (oxygen flux) between permeabilized human MHS and MH-negative (MHN) skeletal muscle fibres with or without prior exposure to halothane. A substrate-uncoupler-inhibitor titration protocol was used to measure the following components of the electron transport chain under conditions of oxidative phosphorylation (OXPHOS) or after uncoupling the electron transport system (ETS): complex I (CI), complex II (CII), complex I and II together (CI+CII) and, as a measure of mitochondrial mass, complex IV (CIV).

Results. Baseline comparisons without halothane exposure showed significantly increased mitochondrial mass (CIV, p=0.021) but lower flux control ratios (FCR) in $CI+CII_{(OXPHOS)}$ and $CII_{(ETS)}$ of MHS mitochondria compared to MHN (p=0.033 and 0.005 respectively) showing that human MHS mitochondria have a functional deficiency. Exposure to halothane triggered a hypermetabolic response in MHS mitochondria significantly increasing mass-specific oxygen flux in $CI_{(OXPHOS)}$, $CI+CII_{(OXPHOS)}$, $CI+CII_{(ETS)}$ and $CII_{(ETS)}$ (p= 0.001 – 0.012), while the rates in MHN samples were unaltered by halothane exposure.

Conclusion. We present evidence of mitochondrial dysfunction in human MHS skeletal muscle both at baseline and after halothane exposure.

Keywords: Malignant hyperthermia; skeletal muscle; mitochondria; electron transport chain

Malignant hyperthermia (MH) is a hypermetabolic reaction triggered by potent inhalation anaesthetics in susceptible individuals [1]. Direct consequences of the hypermetabolic state are increased carbon dioxide production, increased oxygen consumption, metabolic acidosis, and hyperthermia, with reflex sympathetic stimulation [2]. Ultimately skeletal muscle ATP production fails to keep up with energy requirements leading to muscle rigidity and rhabdomyolysis [2]. Variants in the *RYR1* gene that encodes the skeletal muscle calcium release channel (ryanodine receptor, RyR1 [3]) or the *CACNA1S* gene that encodes the sarcolemmal slow voltage gated Ca^{2+} channel which acts as the voltage sensor for excitation-contraction (EC) coupling (dihydropyridine receptor, DHPR [4, 5]) are associated with MH in 76% of UK MH families [6]. Both proteins work in concert to regulate Ca^{2+} levels in skeletal muscle at rest and during EC coupling [7]. Prior to the discovery of genetic linkage between *RYR1* and MH-susceptibility [8, 9], several researchers postulated an important role for mitochondria in the development of an MH reaction. Recent findings in transgenic mice with *RYR1* mutation knock-in has rekindled interest in such a role for mitochondria [10-12]. There is also the implication that mitochondrial dysfunction may explain why some MH susceptible individuals experience myopathic traits such as muscle weakness and exercise intolerance [13].

Some of the earliest observations in MH mitochondria were conducted on the MH porcine model, which showed a halothane-induced inhibition of complex I [14, 15] . Research on *RYR1* mutation knock-in mouse models has found mitochondrial abnormalities with various degrees of severity depending on the *RyR1* mutation. Notable observations have included lower oxidative phosphorylation (OXPHOS), increased oxidative stress and increased reactive oxygen species (ROS) production [10-12]. On a structural level, mitochondrial deformity - an indication of damage - has been observed in multiple reports using electron microscopy. These reports often denote a loss of cristae organization and mitochondrial swelling which suggests there may be metabolic dysfunction and altered OXPHOS in muscles from both MH susceptible mice [10, 16] and humans [17, 18].

In contrast to animal models, research on human MH mitochondrial function is lacking. Despite the structural abnormalities seen in MH susceptible humans [17, 18], evidence for the existence of functional defects is conflicting. Some reports suggest normal OXPHOS and respiratory control in mitochondria of MH susceptible humans

[19], whilst others have claimed impaired OXPHOS and ATP production after bouts of training in MH susceptible individuals [20]. The discrepancies may be explained by variation in sample type, methodology or both. The purpose of this study was to investigate whether mitochondrial dysfunction is present in *ex vivo* skeletal muscle from MH susceptible humans under 1) basal conditions and 2) after halothane exposure.

Methods

Patients

Patients who were considered for inclusion in this study were those attending for investigation of their susceptibility to MH. The reason for investigation was a clinical suspicion of increased risk either because they had had an adverse reaction to anaesthesia consistent with MH or because a family member was known to be MH susceptible. The majority of index case patients had been found not to harbour a pathogenic variant (www.emhg.org) in *RYR1* and *CACNA1S* prior to attending for further investigation, which involved an open muscle biopsy and subsequent *in vitro* contracture testing (IVCT). Family members were either from families where no pathogenic variant had been found or who had been found not to carry a familial variant. Patients gave written informed consent to the study that was approved by Leeds (East) Research Ethics Committee (reference 10/H1306/70).

Patients were diagnosed using the IVCT as either MH susceptible (MHS) or MH negative (MHN) according to the protocol of the European MH Group [21]. The laboratory classification of MHS is subdivided into MHS_{hc} (samples respond abnormally to both caffeine and halothane challenges), MHS_{h} (samples respond normally to caffeine but abnormally to halothane challenge) or MHS_{c} (samples respond abnormally to caffeine but normally to halothane challenge).

Muscle samples

Diagnostic muscle biopsies and IVCTs were conducted according to the protocol of the European MH Group [21]. In brief, six muscle fascicles (typical dimensions 25 mm x 4 mm x 3mm) were excised from *Vastus medialis* under femoral nerve block and immediately placed in oxygenated Krebs' solution (118.1 mM NaCl, 3.4 mM KCl, 0.8 mM $MgSO_4$, 1.2 mM KH_2PO_4, 11.1 mM Glucose, 25.0 mM $NaHCO_3$, 2.5 mM $CaCl_2$, pH 7.4) at room temperature and taken to the MH laboratory. There, the samples were kept at room temperature in the Krebs' solution, which was gassed continuously with carbogen (95% O_2, 5% CO_2), until being used for the IVCT tests. This study required both a muscle fascicle that had not been used for the diagnostic challenge tests (baseline) and a fascicle that had been used in the static halothane test (halothane-exposed). At the end of the halothane test procedure both the halothane-exposed and baseline samples were each placed into 1 ml of ice-cold biopsy preservation buffer, BIOPS (2.77 mM CaK_2EGTA, 7.23 mM K_2EGTA, 5.77 mM Na_2ATP, 6.56 mM $MgCl_2 \cdot 6H2O$, 20 mM taurine, 15 mM Na_2Phosphocreatine, 20 mM imidazole, 0.5 mM dithiothreitol (DTT), and 50 mM MES hydrate, pH 7.1, adjusted with 5 N KOH at 0 °C). The samples were then placed in a petri dish with ice cold BIOPS and separated using sharp forceps to obtain small muscle fibre bundles containing approximately 4-5 fibres each. These samples then underwent chemical permeabilization in BIOPS containing saponin (50 $\mu g \cdot ml^{-1}$) for 30 min, before being washed with 1 ml respiration medium, Mir05 (0.5 mM EGTA, 3 mM $MgCl_2 \cdot 6H2O$, 60 mM lactobionic acid, 20 mM taurine, 10 mM KH_2PO_4, 20 mM HEPES adjusted to pH 7.1 with KOH at 37 °C, 110 mM D-sucrose, and 1 $g \cdot L^{-1}$ essentially fatty acid free BSA) to remove residual saponin. The sample was then taken out of solution and blot-dried for 5 s before being weighed and loaded into the respirometer chambers (5-10 mg in each chamber) containing 2 ml of Mir05. The time between biopsy collection and assay time was approximately 90 – 120 min. This sample preparation procedure was adapted from previously described protocols [22, 23].

High Resolution Respirometry

Oxygen consumption over time was measured using Oroboros respiratory analysers (Oroboros Instruments, Innsbruk, Austria) at 2 s intervals with polarographic oxygen

sensors and expressed as mass-specific oxygen flux (pmol/s*mg). The analyser was calibrated daily in air saturated solution before experimentation. Assays were initiated by injecting oxygen into each chamber to raise the oxygen concentration to > 400 nmol/mL prior to starting a substrate-uncoupler-inhibitor titration (SUIT) protocol. Re-oxygenation of the chambers was performed to maintain oxygen concentration between 200-500 nmol/mL to prevent limitation due to oxygen diffusion [23]. Each assay was performed at 37 °C, with chamber stirrers set at 750 rpm.

SUIT protocol

An adapted SUIT protocol was used to investigate the OXPHOS capacity of individual complexes and respiratory states [22, 23] and is summarised in Figure 1. The procedure was initiated with the addition of 5 μM blebbistatin (BLEB) to prevent spontaneous contraction of muscle fibres [24]. Glutamate (10 mM), malate (0.5 mM) and pyruvate (5 mM) were then applied to facilitate measurements of the complex I respiration in the absence of ADP (LEAK). ADP (2.5 mM) is then added next to allow the measurement of maximal complex I-supported OXPHOS ($CI_{(OXPHOS)}$). At this point the outer mitochondrial membrane integrity was assessed by the addition of 10 μM cytochrome c. An increased respiration rate after addition of cytochrome c indicates outer mitochondrial membrane damage: samples that showed an increased respiration rate after cytochrome c of >10% were excluded from data analysis.

Once membrane integrity has been assessed, the maximal activity of complex II is stimulated with the addition of succinate (10 mM). The oxygen flux at this stage ($CI+CII_{(OXPHOS)}$) reflects the combined activities of complex I and complex II together and is also regarded as the maximum OXPHOS capacity in the coupled state. Next, step-wise additions of carbonyl cyanide 4-(trifluoromethoxy)-phenylhydrazone (FCCP) (0.5 μM) are made until there is no further increase in oxygen flux. This step-wise addition of FCCP uncouples the electron transport system (ETS) by collapsing the proton gradient between the intermembrane space and the mitochondrial matrix providing the maximum ETS capacity ($CI+CII_{(ETS)}$). Then, after uncoupling the system, electron flow through complex I is inhibited using rotenone (0.5 μM), providing maximum complex II activity alone ($CII_{(ETS)}$). Finally, antimycin A is introduced to inhibit complex III. Complex III activity is technically contributing to all

data points aside from the Complex IV assay. However, its activity is not measured directly in this protocol as it obtains electrons downstream of complex I and II. Residual oxygen flux (ROX) present after the addition of antimycin A is a result of non-mitochondrial respiration which is then subtracted from each respiratory state reading before analysis.

Complex IV Assay

Measurement of mass-specific complex IV oxygen flux was used as an alternative proxy marker for estimations of mitochondrial content. Ascorbate (2 mM) and N,N,N′,N′-tetramethyl-p-phenylenediamine (TMPD) (0.5 mM) was applied to each sample at the end of the standard SUIT protocol. The measurement of complex IV flux is taken at the peak of the corresponding trace and residual chemical background is finally removed from this value by applying sodium azide (10 mM) to the sample [25].

Data handling and analysis

Raw data output is in the form of oxygen flux per muscle mass (pmol/s*mg) which includes the confounding effects of both mitochondrial quality and quantity. The data in this study, from samples with and without halothane exposure, were internally normalised to the common reference state, $CI+CII_{(ETS)}$ (maximum uncoupled respiration). Normalised oxygen flux per mass is presented as flux control ratios (FCR) which highlight differences in mitochondrial function, as a proportion of the reference state, which is independent of mitochondrial content.

Oxygen flux readings recorded from each sample trace were exported from proprietary software DatLab5 (Oroboros Instruments, Innsbruk, Austria) into Microsoft Excel before analysis using IBM SPSS statistics v21. Pairwise comparisons were performed using a combination of Wilcoxon signed-rank tests to assess the effects of halothane-exposure and Mann-Whitney U tests to assess median differences between baseline controls. Further analysis using MHS subgroups involved a Kruskal-Wallis test and post hoc Dunn's procedure to identify differences between patients classified as MHN, MHS_h and MHS_{hc}. Data were summarised as boxplots using GraphPad Prism 8. There are no data on the magnitude of changes in OXPHOS variables that are associated with human pathology. Preliminary data from a transgenic mouse model of MH suggested

that there was a standardized mean difference of 0.86 in baseline CI+CII$_{(ETS)}$ between MHS and MHN mice. Such a difference would be detected with a sample size of 12 in each group with $\alpha < 0.05$ and $\beta < 0.2$. We sought to identify changes with a standardized difference in means of >0.75 as this is generally accepted as a relevant effect size in biological systems. On the basis that the MH Unit records more people with MHN compared with MHS diagnoses, we planned to include samples from 23 MHS and at least 35 MHN, in order to achieve $\alpha < 0.05$ and $\beta < 0.2$. This number of samples enables detection of paired (with and without halothane exposure) standardized mean differences of 0.6 and 0.5 for MHS and MHN samples respectively.

Results

Patient characteristics

A summary of patient characteristics is presented in Table 1. Eighteen of the 23 MHS group were subsequently found to carry at least one variant in the *RYR1* gene and these variants are also listed in Table 1. None of the patients had clinical or histopathological features suggestive of a mitochondrial myopathy. We included 59 individuals from 52 families: the maximum number from any family was 2 individuals.

Mass-specific oxygen flux comparisons

Oxygen flux per milligram of muscle was compared between MHN and MHS samples, with or without exposure to halothane (Fig 2). Comparisons of samples without halothane exposure showed no differences between the two phenotypes aside from CIV $_{(MAX)}$ where MHS samples had a significantly greater oxygen flux when compared to MHN (p=0.021), suggesting higher mitochondrial content in the MHS samples. Pairwise comparisons showed that oxygen flux was significantly elevated in MHS samples after halothane exposure in several respiratory states: CI$_{(OXPHOS)}$, CI+CII$_{(OXPHOS)}$, CI+CII$_{(ETS)}$ and CII$_{(ETS)}$ (Table 2). The rates in MHN samples were unaltered by halothane exposure.

Flux control ratios (normalised oxygen flux)

Mass-specific oxygen flux was normalised to a common reference state (control $CI+CII_{(ETS)}$) to generate FCR which removes the confounding effects of mitochondrial content differences among samples (Fig 3). Comparisons of FCR at baseline revealed that $CI+CII_{(OXPHOS)}$ and $CII_{(ETS)}$ were significantly lower in MHS samples when compared to MHN ($p=0.033$ and 0.005, respectively, Table 2), suggesting functional deficiency. Normalised $CIV_{(MAX)}$ showed no significant differences between MHS and MHN controls indicating similar functional capacity of complex IV. In addition, FCR comparisons between control and halothane-exposed samples support the findings seen in the mass-specific dataset, with statistically significant findings in several of the same respiratory states (Table 2). However, one exception was found in MHN $CII_{(ETS)}$ which increased after halothane-exposure ($p=0.041$).

FCR responses within the subdivided MHS phenotypes

FCR were used for further analysis within the MHS phenotype, comparing the magnitude of change with and without exposure to halothane between the MHS_h and MHS_{hc} phenotypes - (Fig 4) – there were no patients in this sample categorized as MHS_c. Results from the Kruskal-Wallis test showed that $CI+CII_{(OXPHOS)}$ responses differed significantly between MH phenotypes after halothane exposure (Table 2). Post hoc analysis showed that these differences in response between MHN and MHS groups is largely attributable to responses of the MHS_{hc} subgroup because we did not find any significant differences in response to halothane exposure between the MHN group and the MHS_h subgroup.

Discussion

Baseline comparisons using mass-specific flux showed a significantly higher $CIV_{(MAX)}$ in MHS compared with MHN muscle, which indicates a greater mass of mitochondria in MHS muscle per milligram of tissue. Alternative mitochondrial markers such as citrate synthase and mtDNA were considered for this study but the complex IV assay was chosen as it can be performed during the experiment and allows measurements on the same exact sample, avoiding issues with degradation. To normalise for differences in mitochondrial mass we compared FCR data which showed that there

were functional deficits in MHS muscle as well. The $CI+CII_{(OXPHOS)}$ and $CII_{(ETS)}$ FCRs were significantly lower in MHS samples compared to MHN which implies that there is uncoupling of mitochondria in MHS muscle in addition to complex II deficiency, both of which would likely result in inefficient ATP production. The uncoupling of MHS mitochondria is perhaps a side effect of the swelling and structural abnormalities seen in previous human studies [18] or it may be a consequence of chronically elevated myoplasmic calcium concentration in MHS muscle (see below). Since no significant differences in $CI_{(OXPHOS)}$ were found, complex II deficiency seems to be the primary cause for the reduced maximum OXPHOS capacity of MHS muscle as defined by $CI+CII_{(OXPHOS)}$ FCR. This is of great importance as a lower OXPHOS capacity suggests that the ETS in MHS mitochondria is less tightly coupled and they are therefore less efficient than MHN mitochondria at producing ATP. Complex II, also known as succinate dehydrogenase, is the only component of the ETS which is encoded entirely by nuclear genes and has roles in both OXPHOS and the Krebs' cycle, indirectly affecting glycolysis [26]. Complex II deficiency has not previously been linked to MH susceptibility and its deficiency may mean that the glycolytic function of MHS muscle is also impaired - a potential area for further research. Collectively these findings may also suggest a potential compensation mechanism, in which MHS muscle upregulates mitochondrial numbers to counteract deficiencies in mitochondrial function, hence similar baseline oxygen flux per unit of muscle mass.

The proposed concept of mitochondrial deficiency in MHS muscle is consistent with that seen in other studies [11,15,20], but some findings are conflicting. An example is the work of Giulivi et al[11], who found a decrease in mitochondrial content, reduced oxygen uptake using malate-glutamate and succinate, and complex I, III and IV deficiency in R163C knock-in mice when compared to wild-types. In contrast, our study showed evidence of human MHS muscle having higher mitochondrial content, deficiency in succinate-facilitated oxygen flux, with activity deficits in complex II only. These discrepancies may be a result of species differences but they could also be explained by differences in methodology. The study of Giulivi and colleagues used isolated mitochondria in the assessment of mitochondrial content and protein complex function, [11] whereas we used permeabilized muscle fibres. Permeabilized muscle allows interplay between the mitochondria, SR and RyR1, which we believe is crucial to accurately assess the biological effects of MH. Furthermore, the oxygen uptake assay

in the mouse study was conducted at 22 °C whereas we used a physiological 37 °C for our experiments: assay temperature significantly impacts OXPHOS capacity [27].

As previously mentioned, one hypothesis for the mitochondrial dysfunction in MHS muscle observed here may be the result of chronic elevation in cytosolic Ca^{2+} that has been demonstrated in human [28] and porcine [29] MH muscle as well as knock-in mouse models [11,12,30]. Ca^{2+} increases mitochondrial activity which can stimulate higher rates of ROS production through complex I, III and, as has been recently shown, complex II of the ETS [31]. Increased ROS production has been observed in MH *RYR1* knock-in mice [11] and it is possible that this may translate into human MHS muscle. Increased ROS production, which can cause DNA damage and structural damage to organelles, could explain the mitochondrial swelling seen in previous electron microscopic studies [10,16,18]. Ca^{2+} is also a positive regulator of the mitochondrial permeability transition pore (MPTP) of the inner mitochondrial membrane [32]. Opening of the MPTP decreases the proton gradient across the inner mitochondrial membrane which is associated with uncoupling of the ETS from OXPHOS [33].

We have also shown that increased activity of several mitochondrial respiratory states is involved in the hypermetabolic response in MHS mitochondria following exposure to halothane. This could simply be a response driven by conversion of myoplasmic ATP to ADP but Diaz-Vegas and colleagues have recently demonstrated a more direct link between skeletal muscle mitochondrial stimulation and activation of RyR1 [34]. This may be the result of sarcoplasmic reticulum Ca^{2+} efflux from the activated RyR1 in MHS muscle and uptake by the mitochondria. Increased intramitochondrial Ca^{2+} stimulates dehydrogenase enzymes which in turn increase NADH and ATP production [35, 36]. The rhabdomyolysis and cell death which occurs in a fulminant MH reaction may partly be caused by the failure of skeletal muscle mitochondria to maintain ATP production to accommodate the Ca^{2+} stimulated state along with apoptotic mechanisms activated by increased intramitochondrial Ca^{2+}. The FCR of MHN $CII_{(ETS)}$ also increased after exposure to halothane, suggesting a non-RyR1 mediated component of this effect of halothane. However, the clinical relevance of this phenomenon is uncertain as it occurs in an artificially uncoupled non-physiological state.

A recent study of Canadian MH susceptible patients found that those who responded abnormally to halothane but not caffeine in the caffeine-halothane contracture test had a higher index of calcium related changes in cultured skeletal muscle cells than patients who responded abnormally to halothane and caffeine [37]. We compared the magnitude of FCR changes in MHS_h and MHS_{hc} fibres and found a significantly greater effect of halothane exposure on ($CI+CII_{(OXPHOS)}$) in MHS_{hc} muscle, which is what we expected, although it is at odds with what might have been anticipated from the work of Figueroa and colleagues [37]. This potential discrepancy might be explained by the use of cultured myotubes by Figueroa and colleagues whereas we studied adult muscle fibres.

Another unexpected observation was the lack of change in $CI_{(OXPHOS)}$ after halothane treatment. Complex I activity was reduced by halothane in MH pigs [11, 12] but research in other models has suggested this effect is independent of the MH trait. Porcine heart mitochondria have shown reversible dose-dependent inhibition of complex I (NADH oxidoreductase) after exposure to isoflurane, sevoflurane and halothane – the latter of which proved to be the most potent among them [38]. Research using the complex I mutant *gas-1 C.elegans* model has also shown evidence of decreased complex I function and increased sensitivity to the application of potent inhalation anaesthetics [39, 40]. This was not observed in our MHS or MHN muscle and may be due to the inhibitory effects of halothane on complex I being both acute and reversible. Such changes would not be detected using our protocol because of the time delay between halothane exposure and measurement of mitochondrial function (~90 -120 min). In addition, previous studies with halothane treatment have used isolated mitochondria taken out of the normal cellular environment[11,12].

The time delay between halothane exposure and measurement of mitochondrial function might also have reduced the magnitude of change in other components of the ETS and could have obscured other acute and reversible changes. It is also possible that the permeabilization of the muscle fibres, which is necessary for the SUIT protocol, might have limited the responses to halothane exposure. A further potential confounding factor in our study was that the halothane-exposed samples were maintained at approximate physiological length and tension as well as being electrically stimulated during the halothane contracture test, whereas the baseline samples were not. While we think it may be that the differences observed between our

halothane-exposed and baseline samples are a result of the halothane exposure rather than the other interventions, we were unable to demonstrate this because of a limited supply of human muscle tissue. We plan to address this in future studies using muscle tissue from *RYR1* knock-in mouse models.

In conclusion, we have demonstrated evidence of impaired mitochondrial function in permeabilised human MHS skeletal muscle and we hypothesise that this results from chronic elevation of cytoplasmic Ca^{2+} in MHS muscle that causes mitochondrial uncoupling and structural damage through increased ROS production. Exposure to 2% halothane significantly increased OXPHOS and ETS capacity in MHS muscle, confirming a hypermetabolic response to halothane in MHS mitochondria with functional deficiency at baseline.

Contribution of authors

Conception and design of the study: PMH, MAS, JPB
Conduct of experiments and data collection: LC, JPB
Data analysis & interpretation: all authors
Drafting of manuscript: LC, PMH
All authors reviewed drafts of the manuscript and approved the final version

Disclosure of funding sources:

BJA/RCoA PhD studentship (MAS & PMH)
National Institutes of Health (NIH): National Institute of Arthritis, Musculoskeletal and Skin Diseases (2P01 AR-05235; PMH, PDA)

Declaration of interests

PMH is an Editorial Board Member of BJA.

References

1. Hopkins PM. Malignant hyperthermia – pharmacology of triggering. *Br J Anaesth* 2011; **107**:48-56
2. Hopkins PM. Malignant hyperthermia: advances in clinical management and diagnosis. *Br J Anaesth* 2000; **85**:118-28
3. Zorzato F, Fujii J, Otsu K, et al. Molecular cloning of cDNA encoding human and rabbit forms of the Ca2+ release channel (ryanodine receptor) of skeletal muscle sarcoplasmic reticulum. *J Biol Chem* 1990; **265**:2244-56
4. Weiss RG, O'Connell KM, Flucher BE, Allen PD, Grabner M, Dirksen RT. Functional analysis of the R1086H malignant hyperthermia mutation in the DHPR reveals an unexpected influence of the III-IV loop on skeletal muscle EC coupling. *Am J Physiol Cell Physiol* 2004; **287**:C1094-102
5. Eltit JM, Bannister RA, Moua O, et al. Malignant hyperthermia susceptibility arising from altered resting coupling between the skeletal muscle L-type Ca2+ channel and the type 1 ryanodine receptor. *Proc Natl Acad Sci USA* 2012; **109**:7923-8
6. Miller DM, Daly C, Aboelsaod EM, et al. Genetic epidemiology of malignant hyperthermia in the United Kingdom. *Br J Anaesth* 2018; **121**:944-52
7. Hernández-Ochoa EO, Pratt SJP, Lovering RM, Schneider MF. Critical Role of Intracellular RyR1 Calcium Release Channels in Skeletal Muscle Function and Disease. *Front Physiol* 2015; **6**:420
8. MacLennan DH, Duff C, Zorzato F, et al. Ryanodine receptor gene is a candidate for predisposition to malignant hyperthermia. *Nature* 1990; **343**:559–61
9. McCarthy TV, Healy JM, Heffron JJ, et al. Localization of the malignant hyperthermia susceptibility locus to human chromosome 19q12-13.2. *Nature* 1990; **343**:562-4
10. Durham WJ, Aracena-Parks P, Long C, et al. RyR1 S-nitrosylation underlies environmental heat stroke and sudden death in Y522S RyR1 knockin mice. *Cell* 2008; **133**:53-65
11. Giulivi C, Ross-Inta C, Omanska-Klusek A, et al. Basal bioenergetic abnormalities in skeletal muscle from ryanodine receptor malignant hyperthermia-susceptible R163C knock-in mice. *J Biol Chem* 2011; **286**:99-113
12. Yuen B, Boncompagni S, Feng W, et al. Mice expressing T4826I-RYR1 are viable but exhibit sex- and genotype-dependent susceptibility to malignant hyperthermia and muscle damage. *FASEB J* 2012; **26**:1311-22
13. Riazi S, Kraeva N, Hopkins PM. Malignant hyperthermia in the post-genomics era: new perspectives on an old concept. *Anesthesiology* 2018;**128**:168-80

14. Britt BA, Endrenyi L, Cadman DL, Fan HM, Fung HY. Porcine malignant hyperthermia: effects of halothane on mitochondrial respiration and calcium accumulation. *Anesthesiology* 1975; **42**:292-300
15. Gronert GA, Heffron JJ. Skeletal muscle mitochondria in porcine malignant hyperthermia: respiratory activity, calcium functions, and depression by halothane. *Anesth Analg* 1979; **58**:76-81
16. Boncompagni S, Rossi AE, Micaroni M, et al. Mitochondria are linked to calcium stores in striated muscle by developmentally regulated tethering structures. *Mol Biol Cell* 2009; **20**:1058-67
17. Isaacs H, Heffron JJ, Badenhorst M. Predictive tests for malignant hyperpyrexia. *Br J Anaesth* 1975; **47**:1075-80
18. Lavorato M, Gupta PK, Hopkins PM, Franzini-Armstrong C. Skeletal muscle microalterations in patients carrying malignant hyperthermia-related mutations of the e-c coupling machinery. *Eur J Transl Myol* 2016; **26**:6105
19. Cheah KS, Cheah AM, Fletcher JE, Rosenberg H. Skeletal muscle mitochondrial respiration of malignant hyperthermia-susceptible patients. Ca2+-induced uncoupling and free fatty acids. *Int J Biochem* 1989; **21**:913-20.
20. Thompson SJ, Riazi S, Kraeva N, et al. Skeletal muscle metabolic dysfunction in patients with malignant hyperthermia susceptibility. *Anesth Analg* 2017; **125**:434-441
21. Hopkins PM, Rüffert H, Snoeck MM, et al. European Malignant Hyperthermia Group guidelines for investigation of malignant hyperthermia susceptibility. *Br J Anaesth* 2015; **115**:531-9
22. Kuznetsov AV, Veksler V, Gellerich FN, Saks V, Margreiter R, Kunz WS. Analysis of mitochondrial function in situ in permeabilized muscle fibers, tissues and cells. *Nat Protoc* 2008; **3**:965-76
23. Pesta D, Gnaiger E. High-resolution respirometry: OXPHOS protocols for human cells and permeabilized fibers from small biopsies of human muscle. *Methods Mol Biol* 2012; **810**:25-58
24. Perry CG, Kane DA, Herbst EA, et al. Mitochondrial creatine kinase activity and phosphate shuttling are acutely regulated by exercise in human skeletal muscle. *J Physiol* 2012; **590**:5475-86
25. Larsen S, Nielsen J, Hansen CN et al. Biomarkers of mitochondrial content in skeletal muscle of healthy young human subjects. *J Physiol* **2012,** *590*:3349-60
26. Bezawork-Geleta A, Rohlena J, Dong L, Pacak K, Neuzil J. Mitochondrial complex II: At the crossroads. *Trends Biochem Sci* 2017; **42**:312-325

27. Lemieux H, Blier PU, Gnaiger E. Remodeling pathway control of mitochondrial respiratory capacity by temperature in mouse heart: electron flow through the Q-junction in permeabilized fibers. *Sci Rep* 2017; **7**:2840
28. López JR, Alamo L, Caputo C, Wikinski J, Ledezma D. Intracellular ionized calcium concentration in muscles from humans with malignant hyperthermia. *Muscle & Nerve* 1985; **8**:355-8
29. Lopez JR, Alamo LA, Jones DE, et al. [Ca2+]i in muscles of malignant hyperthermia susceptible pigs determined in vivo with Ca2+ selective microelectrodes. *Muscle & Nerve* 1986; **9**:85-86
30. Lopez JR, Kaura V, Diggle CP, Hopkins PM, Allen PD. Malignant hyperthermia, environmental heat stress and intracellular calcium dysregulation in a mouse model expressing the p.G2435R variant of the *RYR1* gene. *Br J Anaesth* 2018; 121:953-61
31. Guzy RD, Sharma B, Bell E, Chandel NS, Schumacker PT. Loss of the SdhB, but not the SdhA, subunit of complex II triggers reactive oxygen species-dependent hypoxia-inducible factor activation and tumorigenesis. *Mol Cell Biol* 2008; **28**:718-31
32. Szabo I, Zoratti M. Mitochondrial channels: ion fluxes and more. *Physiol Rev* 2014; **94**:519-608
33. Mailloux RJ, Harper ME. Mitochondrial proticity and ROS signaling: lessons from the uncoupling proteins. *Trends Endocrinol Metab* 2012; **23**:451-8
34. Díaz-Vegas AR, Cordova A, Valladares D, et al. Mitochondrial calcium increase induced by RyR1 and IP3R channel activation after membrane depolarization regulates skeletal muscle metabolism. *Front Physiol* 2018; **9**:791
35. McCormack JG, Denton RM. The effects of calcium ions and adenine nucleotides on the activity of pig heart 2-oxoglutarate dehydrogenase complex. *Biochem J* 1979; **180**:533-44
36. Griffiths EJ, Rutter GA. Mitochondrial calcium as a key regulator of mitochondrial ATP production in mammalian cells. *Biochim Biophys Acta* 2009; **1787**:1324-33
37. Figueroa L, Kraeva N, Manno C, Toro S, Ríos E, Riazi S. Abnormal calcium signalling and the caffeine–halothane contracture test. *Br J Anaesth* Advance Access published on September 20, 2018, doi: 10.1016/j.bja.2018.08.009
38. Hanley PJ, Ray J, Brandt U, Daut J. Halothane, isoflurane and sevoflurane inhibit NADH:ubiquinone oxidoreductase (complex I) of cardiac mitochondria. *J Physiol* 2002; **544**:687-93
39. Kayser EB, Morgan PG, Sedensky MM. Mitochondrial complex I function affects halothane sensitivity in Caenorhabditis elegans. *Anesthesiology* 2004; **101**:365-72
40. Falk MJ, Kayser EB, Morgan PG, Sedensky MM. Mitochondrial complex I function modulates volatile anesthetic sensitivity in C. elegans. *Curr Biol* 2006; **16**:1641-5

Table 1

***In vitro* contracture test result**	**MHN (n = 36)**	**MHS (n = 23)**					
		MHS_h (n = 12)			**MHS_{hc} (n = 11)**		
Male: Female	16: 20	5: 7			7: 4		
Age at biopsy (years)	(11 – 68)	(12 – 64)			(12 – 57)		
Individuals with at least one *RYR1* variant	-	8			10		
***RYR1* variants found**	-	**Nucleotide change**	**Amino acid change**	**Accession number**	**Nucleotide change**	**Amino acid change**	**Accession number**
		c.251C>T[b]	p.Thr84Met	rs186983396	c.455C>A[b]	p.Ala152Asp	-
		c.4178A>G[a]	p.Lys1393Arg	rs137933390	c.1202G>A[c]	p.Arg401His	rs193922766
		c.5183C>T[c]	p.Ser1728Phe	rs193922781	c.8729C>T[b]	p.Tyr2910Met	-
		c.6670C>T[b]	p.Arg2224Cys	rs199870223	c.10357C>T[b]	p.Arg3453Cys	rs1482429489
		c.6785G>A[b]	p.Gly2262Asp	-	c.11132C>T[c]	p.Thr3711Met	rs375915752
		c.7879G>A[c]	p.Val2627Met	-	c.11958C>G[c]	p.Asp3986Glu	rs193922842
		c.12860C>T[b]	p.Ala4287Val	-	c.12700G>C[c]	p.Val4234Leu	rs193922852
		c.14210G>A[c]	p.Arg4737Gln	rs193922868	c.7879G>A[c]	p.Val2627Met	-
		c.4293G>A	p.Thr1431=	rs727504130	c.1021G>A[d]	p.Gly341Arg	rs121918592

Table 1. Summary of characteristics of the patients contributing samples for this study. MHN= malignant hyperthermia negative; MHS = malignant hyperthermia susceptible; MHS_h = abnormal response in the *in vitro* contracture test to halothane but not caffeine; MHS_{hc} = abnormal response in the *in vitro* contracture test to halothane and caffeine. The *RYR1* variants are annotated for their likely

pathogenicity using the criteria of Miller et al[6] as: a. Unlikely pathogenic; b. Potentially pathogenic; c. Likely pathogenic; d. pathogenic. IVCT contracture data for each MHS individual is available in supplementary table 1.

Table 2

Respiratory State	Oxygen consumption rate (pmol/s*mg)		
	MHN	MHS	MHN vs MHS
	Control vs halothane-exposure (p value)		Control comparisons (p value)
LEAK	0.944	0.429	0.732
$CI_{(OXPHOS)}$	0.593	**0.012**	0.113
$CI+CII_{(OXPHOS)}$	0.789	**0.005**	0.071
$CI+CII_{(ETS)}$	0.157	**0.003**	0.050
$CII_{(ETS)}$	0.057	**0.001**	0.376
$CIV_{(MAX)}$	0.718	0.101	**0.021**

Respiratory State	Flux control ratio (FCR)		
	MHN	MHS	MHN vs MHS
	Control vs halothane-exposure (p value)		Control comparisons (p value)
LEAK	0.753	0.362	0.074
$CI_{(OXPHOS)}$	0.480	**0.007**	0.534
$CI+CII_{(OXPHOS)}$	0.470	**0.003**	**0.033**
$CI+CII_{(ETS)}$			
$CII_{(ETS)}$	**0.041**	**0.001**	**0.005**
$CIV_{(MAX)}$	0.307	0.052	0.913

Respiratory State	FCR Differences (Halothane-exposed - control)			
	Kruskal-Wallis (p value)	*Post Hoc* (p value)		
		MHN vs MHS_h	MHN vs MHS_{hc}	MHS_h vs MHS_{hc}
LEAK	0.349			
$CI_{(OXPHOS)}$	0.209			
$CI+CII_{(OXPHOS)}$	**0.043**	1.000	**0.036**	0.390
$CI+CII_{(ETS)}$	0.086			
$CII_{(ETS)}$	0.263			
$CIV_{(MAX)}$	0.532			

Table 2. Summary of all statistical comparisons for each data set, outlining the specific p values for each pairwise comparison between and within phenotype for the mass-specific oxygen flux (pmol/s*mg) and FCR readings. The p values for FCR differences between MHS subgroups are also included with *post hoc* statistics for each comparison. MHN= malignant hyperthermia negative; MHS = malignant

hyperthermia susceptible; MHSh = abnormal response in the *in vitro* contracture test to halothane but not caffeine; MHS_{hc} = abnormal response in the *in vitro* contracture test to halothane and caffeine.

Legends to Figures

Fig 1. Example high resolution respirometry trace showing the rate of oxygen flux (red line) over time after sequential titration of substrates and inhibitors, expressed as pmol/s*mg. The blue line represents oxygen levels within the chamber (nmol/ml). Vertical dashed lines represent timepoints where substrates have been added. The horizontal black lines which overlay the red line plateaus indicate the position of data points.

Fig 2. High resolution respirometry of permeabilised *Vastus medialis* biopsies from MHN (n = 36) and MHS (n = 23) individuals. Boxplots show median, IQR and min-max range for each phenotype in control and halothane-exposed samples. Statistically significant pairwise comparisons ($p<0.05$) are labelled with an asterisk (refer to table 2 for exact p values). MHN= malignant hyperthermia negative; MHS = malignant hyperthermia susceptible.

Fig 3. Boxplot comparison of flux control ratios (FCR) from MHN (n = 36) and MHS (n = 23) control and halothane-exposed samples. FCR are generated by internally normalizing oxygen flux per muscle mass to the non-halothane-exposed control $CI+CII_{(ETS)}$ (indicated by the horizontal dashed line). Boxplots show median, IQR and min-max range for each phenotype in control and halothane-exposed samples. Statistically significant pairwise comparisons ($p<0.05$) are labelled with an asterisk (refer to table 2 for exact p values). MHN= malignant hyperthermia negative; MHS = malignant hyperthermia susceptible.

Fig 4. Boxplot comparison showing the change flux control ratios (FCR) (halothane-exposed - control) for each respiratory state. MHN samples (n = 36) were plotted with MHS samples (n = 23) - further split into MHS_h (n = 12) and MHS_{hc} (n = 11) subgroups. Boxplots show median, IQR and min-max response range for each phenotype. Comparisons labelled with an asterisk show statistically significant post hoc pairwise comparisons (refer to table 2 for exact p values). MHN= malignant hyperthermia negative; MHS = malignant hyperthermia susceptible; MHS_h = abnormal response in

the *in vitro* contracture test to halothane but not caffeine; MHS_{hc} = abnormal response in the *in vitro* contracture test to halothane and caffeine

Figure 1

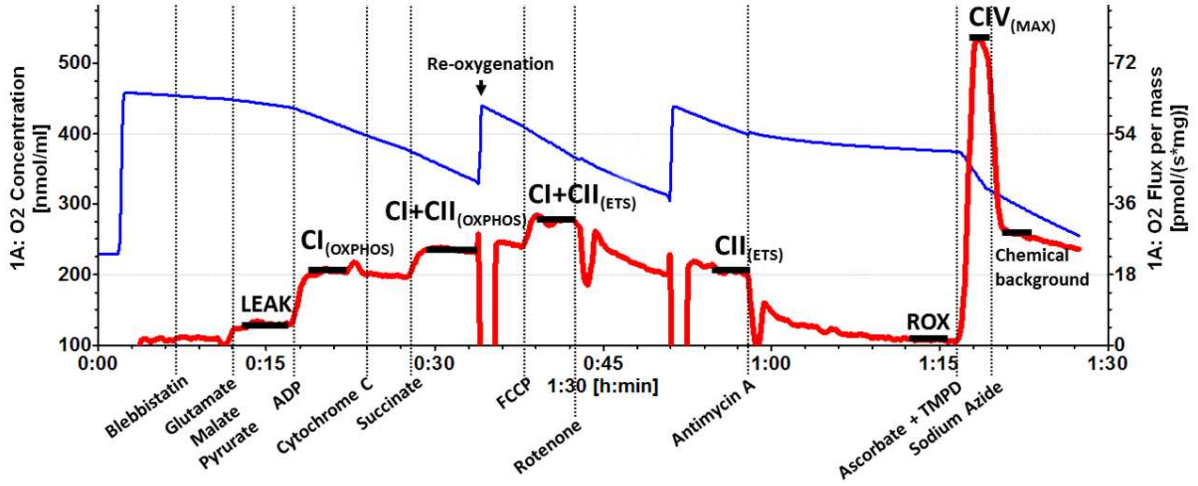
1A: O2 Concentration [nmol/ml]
1A: O2 Flux per mass [pmol/(s*mg)]
500
400
300
200
100
72
54
36
18
0
0:00
0:15
0:30
0:45
1:00
1:15
1:30
1:30 [h:min]
Re-oxygenation
LEAK
CI(OXPHOS)
CI+CII(OXPHOS)
CI+CII(ETS)
CII(ETS)
ROX
CIV(MAX)
Chemical background
Blebbistatin
Glutamate
Malate
Pyrurate
ADP
Cytochrome C
Succinate
FCCP
Rotenone
Antimycin A
Ascorbate + TMPD
Sodium Azide

Figure 2

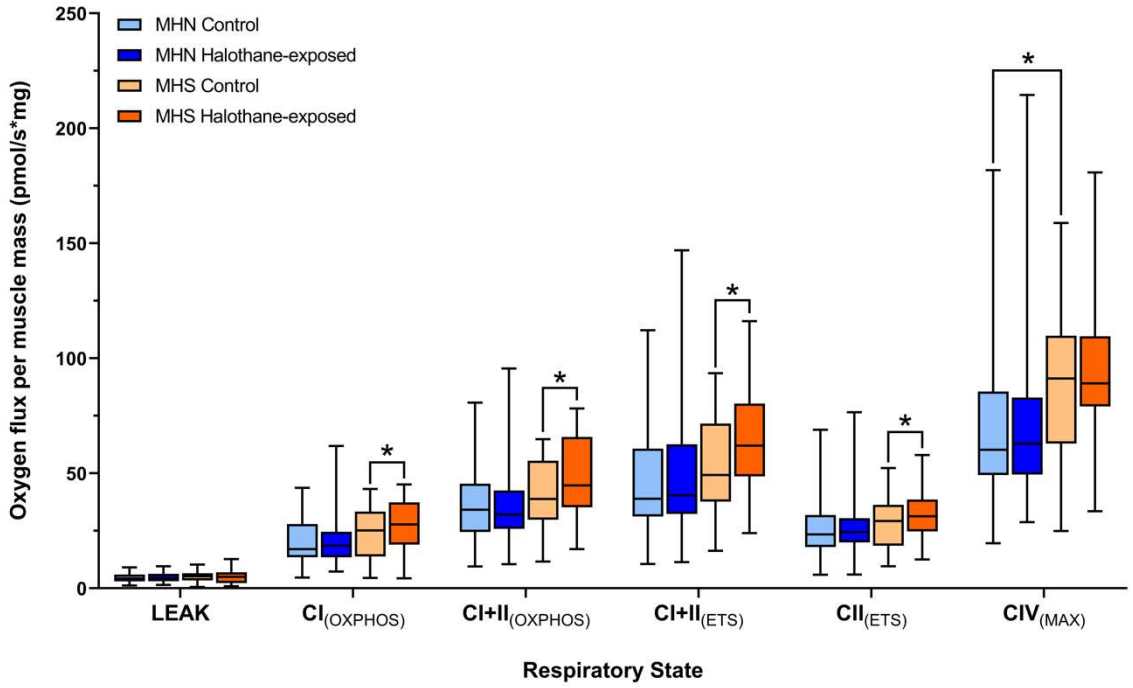
MHN Control
MHN Halothane-exposed
MHS Control
MHS Halothane-exposed
Oxygen flux per muscle mass (pmol/s*mg)
250
200
150
100
50
0
*
*
*
*
*
LEAK
CI(OXPHOS)
CI+II(OXPHOS)
CI+II(ETS)
CII(ETS)
CIV(MAX)
Respiratory State

Figure 3

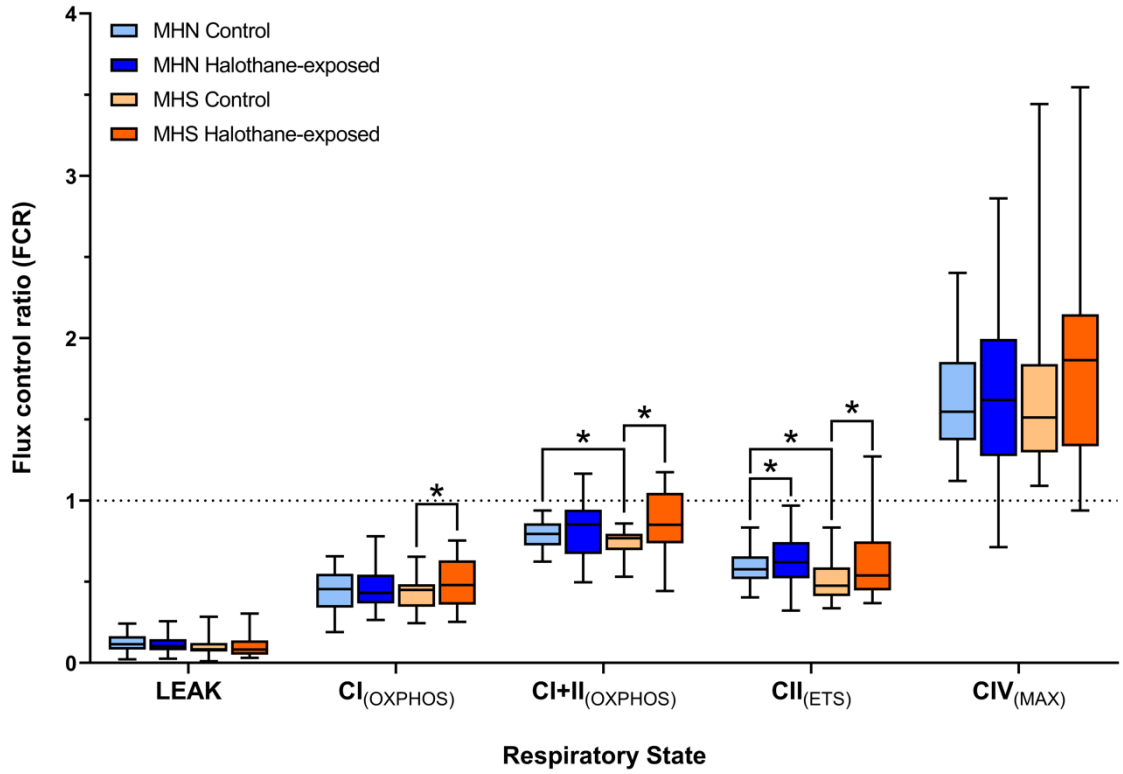
MHN Control
MHN Halothane-exposed
MHS Control
MHS Halothane-exposed
Flux control ratio (FCR)
0
1
2
3
4
*
LEAK
CI(OXPHOS)
CI+II(OXPHOS)
CII(ETS)
CIV(MAX)
Respiratory State

Figure 4

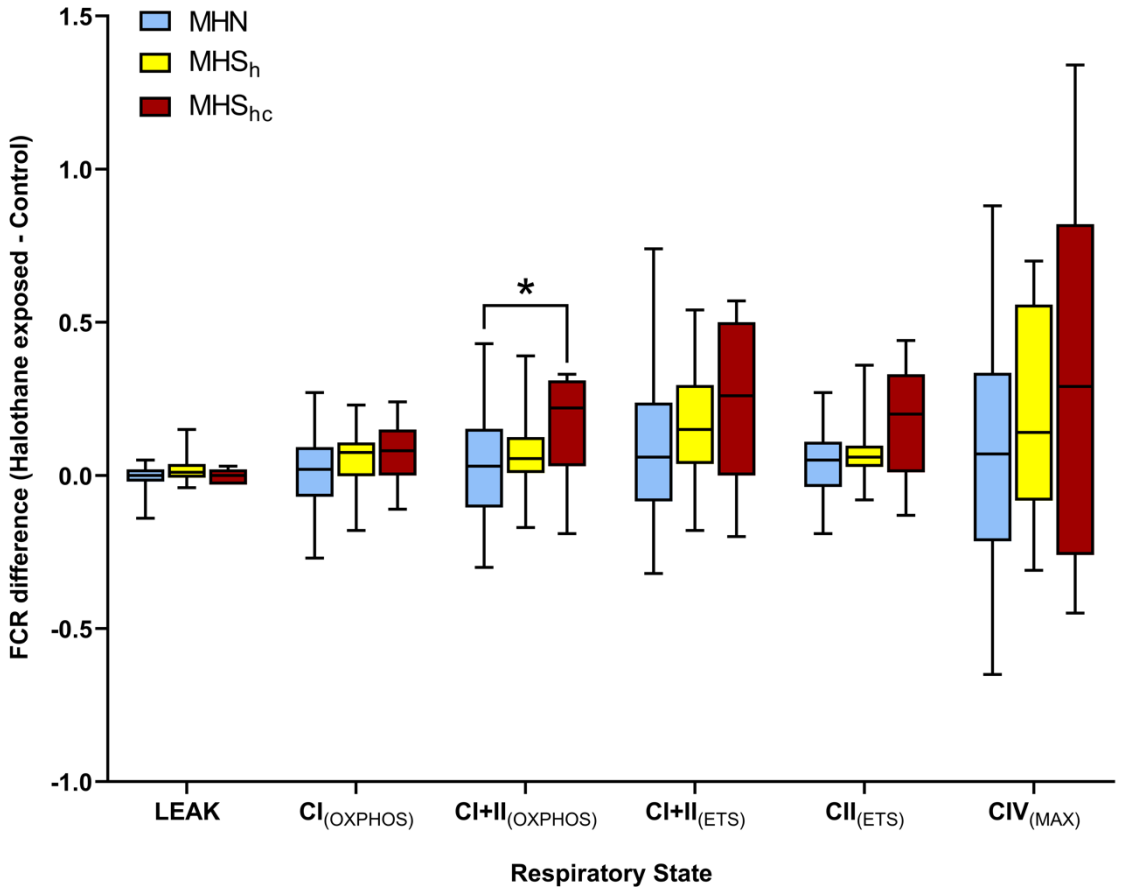
MHN
MHSh
MHShc
FCR difference (Halothane exposed - Control)
1.5
1.0
0.5
0.0
-0.5
-1.0
*
LEAK
CI(OXPHOS)
CI+II(OXPHOS)
CI+II(ETS)
CII(ETS)
CIV(MAX)
Respiratory State

Supplementary Table 1

Patient number	IVCT classification	Contracture at 2% halothane (g)	Contracture at 2 mM caffeine (g)
1	MHS_h	0.6	0
2	MHS_h	0.4	0
3	MHS_h	1.05	0
4	MHS_h	0.3	0
5	MHS_h	0.35	0
6	MHS_h	0.2	0
7	MHS_h	0.2	0
8	MHS_h	0.3	0
9	MHS_h	0.2	0.05
10	MHS_h	0.3	0
11	MHS_h	0.2	0.1
12	MHS_h	0.2	0.1
13	MHS_{hc}	0.7	0.2
14	MHS_{hc}	0.7	2.0
15	MHS_{hc}	1.8	1
16	MHS_{hc}	1.05	0.5
17	MHS_{hc}	0.9	0.2
18	MHS_{hc}	1.05	0.75
19	MHS_{hc}	2.55	0.9
20	MHS_{hc}	0.4	0.25
21	MHS_{hc}	1.6	0.4
22	MHS_{hc}	0.9	0.2
23	MHS_{hc}	0.45	0.3

In vitro contracture test (IVCT) responses at 2% halothane and 2 mM caffeine for the malignant hyperthermia susceptible patients. The malignant hyperthermia negative patients all had 0 g responses at 2% halothane and 2 mM caffeine. MHS_h = abnormal response in the *in vitro* contracture test to halothane but not caffeine; MHS_{hc} = abnormal response in the *in vitro* contracture test to halothane and caffeine.